Thermal Stability of Peroxynitrates

F. KIRCHNER,* A. MAYER–FIGGE, F. ZABEL,** K. H. BECKER

Bergische Universität-Gesamthochschule Wuppertal, Physikalische Chemie/FB 9, Gauss-Str. 20, 42097 Wuppertal, Germany

Received 14 November 1997; accepted 20 August 1998

ABSTRACT: Peroxynitrates are thermally unstable intermediates (at ambient temperatures) in the atmospheric degradation of hydrocarbons. In this work, thermal lifetimes of nine peroxynitrates have been measured as a function of temperature and, for two of them, also, as a function of total pressure. In the presence of excess NO, relative concentrations of the peroxynitrates were followed in a 420 l reaction chamber as a function of time by means of long-path IR absorption using a Fourier transform spectrometer. Original data on the unimolecular decomposition rate constants are presented for the peroxynitrates RO_2NO_2 with R = C_6H_{11}, $CH_3C(O)CH_2$, $C_6H_5CH_2$, CH_2I, $CH_3C(O)OC(H)CH_3$, $C_6H_5OCH_2$, $(CH_3)_2NC(O)$, $C_6H_5OC(O)$, and $C_2H_5C(O)$. Thermal lifetimes at room temperature and atmospheric pressure are very short (in the order of seconds) for substituted methyl peroxynitrates (i.e., $R'CH_2O_2NO_2$) but rather long for substituted formyl peroxynitrates (i.e., $R''C(O)O_2NO_2$). Kinetic data from this and previous work from our laboratory are used to derive structure-stability relationships which allow an estimate of the thermal lifetimes of peroxynitrates from readily available ^{13}C n.m.r. shift data.
 Int J Chem Kinet 31: 127–144, 1999

INTRODUCTION

Peroxynitrates (RO_2NO_2) are common intermediates in the atmospheric degradation of hydrocarbons:

$$RH + OH \longrightarrow R + H_2O \quad (1)$$
$$R + O_2\ (+M) \longrightarrow RO_2\ (+M) \quad (2)$$
$$RO_2 + NO_2\ (+M) \longrightarrow RO_2NO_2\ (+M) \quad (3)$$

The most important tropospheric loss process of peroxynitrates is thermal decomposition,

$$RO_2NO_2\ (+M) \longrightarrow RO_2 + NO_2\ (+M), \quad (-3)$$

followed by the reaction of RO_2 radicals with NO, NO_3, HO_2, or RO_2. The more stable peroxynitrates (e.g., $CH_3C(O)O_2NO_2$ (= PAN), $C_2H_5C(O)O_2NO_2$) act as temporary reservoirs of NO_x. They can transport NO_x over large distances from polluted to unpolluted areas [1,2], thus, contributing to ozone formation in remote areas.

At present, only acyl peroxynitrates are known to be stable enough to accumulate to measurable mixing ratios in the tropospheric boundary layer [3–7]. Contrary to this, alkyl peroxynitrates are quite unstable, with thermal lifetimes of the order of seconds at room temperature and atmospheric pressure [8,9]. Substitution of one or more H atoms in $CH_3O_2NO_2$ by halogen atoms or other electron withdrawing groups, however, leads to considerably longer thermal lifetimes [4–8,10].

In this article, the thermal decomposition of RO_2NO_2 is investigated for R = C_6H_{11}, $CH_3C(O)CH_2$, $C_6H_5CH_2$, CH_2I, $CH_3C(O)OC(H)CH_3$, $C_6H_5OCH_2$, $(CH_3)_2NC(O)$, $C_6H_5OC(O)$, and $C_2H_5C(O)$. Several of these peroxynitrates are of interest with respect to the atmospheric degradation mechanisms of important

Present address: Ecole Polytechnique Fédérale de Lausanne, DGR-LPAS, CH-1015 Lausanne

**Present address:* Institut f. Physikal. Chemie, Universität Stuttgart, Pfaffenwaldring 55, D-70550 Stuttgart

Correspondence to: F. Zabel

Contract grant sponsor: EC (European Commission)

Contract grant number: contract no. EV5V-0024

Contract grant sponsor: Bundesminister für Bildung, Wissenschaft, Forschung und Technologie (BMBF)

 CCC 0538-8066/99/020127-18

precursors (i.e., acetone, toluene, and propane). The other peroxynitrates have been studied in order to complement the data base for establishing structure-stability relationships which allow to estimate thermal lifetimes of peroxynitrates from tabulated ^{13}C n.m.r. data. The basic idea of this method is the observed strong correlation between the ROO—NO_2 bond energy in peroxynitrates and the electron drawing capability of R, where R contains a C atom which is attached to the peroxynitrate group. Since for this C atom both the electron distribution in its vicinity and its ^{13}C n.m.r. shift depend on the electronegativity of its substituents, it is reasonable to assume that there exists a correlation between the ROO—NO_2 bond energy and the ^{13}C n.m.r. shift of the carbon atom which is directly bonded to the peroxy group. The experimental data of the present and previous work from this laboratory are used to establish such a correlation.

EXPERIMENTAL

The experiments were performed in a 420 IL reaction chamber made of DURAN glass which is temperature controlled between 243 and 323 K and surrounded by 20 fluorescent lamps for the photolytic generation of radicals with light of $\lambda \geq 300$ nm. This apparatus has been described elsewhere in greater detail [11]. RO_2NO_2, NO, and NO_2 were detected in situ as a function of time by long-path (50.4 m) FTIR spectrometry using a White multireflection mirror system.

Except for $CH_2IO_2NO_2$, peroxynitrates were produced by photolysis of $RH/Cl_2/O_2/NO_2/N_2$ mixtures at $\lambda \geq 300$ nm, according to the following mechanism:

$$Cl_2 + h\nu \longrightarrow 2\ Cl \qquad (4)$$

$$RH + Cl \longrightarrow R + HCl, \qquad (5)$$

followed by reactions (2) and (3). Partial pressures of O_2 were ≥ 2 mbar. $CH_2IO_2NO_2$ was generated by photolysis of CH_2I_2 at $\lambda \geq 300$ nm in the presence of O_2 and NO_2. After measuring the first-order wall loss rate constant of RO_2NO_2, a large excess of NO (0.2–0.3 mbar) was added to the reaction chamber. Under these conditions, peroxy radicals irreversibly react with NO,

$$RO_2 + NO \longrightarrow \text{products}, \qquad (6)$$

and reaction (3) cannot compete with reaction (6). Therefore, the difference of the first-order decay rate constants of RO_2NO_2 before and after NO addition corresponds to the unimolecular gas-phase decomposition rate constant k_{-3}.

During thermal decomposition of RO_2NO_2 in the dark, alkyl radicals R′ can be generated. In addition to adding to O_2, R′ can react with Cl_2 to produce R′Cl and Cl, thus, liberating Cl atoms. Cl atoms can undergo a variety of reactions including the reaction with RO_2NO_2 which would affect the measured decomposition rate constants of RO_2NO_2. An estimate of the relative rates for the reactions of R′ with Cl_2 and O_2 and for the reactions of Cl atoms with other reaction partners showed that the loss of RO_2NO_2 due to reaction with Cl is considerably less than 10% of its loss due to thermal decomposition, in particular because: (i) the reaction of the alkyl radicals with O_2 effectively competes with the Cl_2 reaction and (ii) most of the Cl atoms are scavenged in the fast reactions with NO and NO_2 both of which are present in high concentrations.

RESULTS AND DISCUSSION

Evaluation of Kinetic Data

Usually, the IR absorption band selected for the data evaluation of a certain peroxynitrate disappeared according to a first-order rate law after the addition of excess NO. In addition to the peroxynitrate, organic nitroso compounds, nitrites, and nitrates can, also, be formed in the course of the reaction both during the photolysis and the thermal decomposition of the peroxynitrate in the dark. In most cases, these absorptions do not interfere with the peroxynitrate absorption band which was used for data evaluation. In some cases, however, a residual absorption was observed at the position of this band after completion of the decomposition of the peroxynitrate. Two simple cases may be considered: (i) The residual absorption is formed during the photolysis period and remains constant during the thermal decomposition of RO_2NO_2 in the dark and (ii) The residual absorption builds up during the thermal decomposition of RO_2NO_2 in the dark with the same time constant as the thermal decomposition. In both cases (i) and (ii), evaluation of the absorptions which were obtained by subtraction of the residual from the measured total absorptions according to a first-order rate law gives the correct rate constant k_{-3}. Possible deviations from the assumptions (i) and (ii) were investigated in detail whenever there was evidence for interfering absorptions, and errors arising from these interferences were considered to be minor.

The temperature dependence of k_{-3} can be described by the Arrhenius expression

$$\ln k = \ln A - E_a/RT \qquad (1)$$

At room temperature, small errors of the activation energy E_a cause large errors in the preexponential factor A. If only a small temperature range is experimentally available or the rate constants are scattered, rather high error limits are obtained for E_a implying huge error limits for A. In earlier work from this laboratory which was based on more extensive data sets, preexponential factors between 2×10^{15} and 2×10^{17} s^{-1} were derived experimentally whenever the corresponding decomposition was not very far from the high-pressure limit [5,7]. In addition, there was evidence [5] that the preexponential factors rise with increasing activation energy. The measured preexponential factors of substituted methyl peroxynitrates ranged from 3×10^{15} to 3×10^{16} s^{-1}, with a geometric mean value of 1×10^{16} s^{-1}. For this reason, $A = 1.0 \times 10^{16}$ s^{-1} has been assumed in the present work for peroxynitrates of the structure $R'CH_2O_2NO_2$ whenever the experimental data did not allow the accurate determination of A directly from the temperature dependence of k_{-3}. In order to determine reasonable error limits for the activation energies, the lowest and highest values of A obtained experimentally for different RO_2NO_2 were multiplied by factors of 1/3 and 3, respectively, with the purpose of obtaining reliable lower and upper limits for A, i.e., $\log (A/s^{-1}) = 16.0 \pm 1.0$ was assumed. The activation energies which have to be used to fit the measured rate constant of a particular RO_2NO_2 at the mean temperature of the experiments by employing these lower and upper limits of A are then identified as the upper and lower limits of E_a, respectively. The stated error limits of E_a are either these values or the 2σ error of the experimental Arrhenius plot whichever of these figures is smaller. The contribution of the error of k_{-3} (usually less than 20%) to the uncertainty of the activation energy is less important (≤ 0.4 kJ mol^{-1}) as compared with the error related to the uncertainty of the A factor. For substituted formyl peroxynitrates, the range of experimentally determined A factors was from 5×10^{15} to 1.6×10^{17} s^{-1} [5,7], with a geometric mean of about 3×10^{16} s^{-1}. The estimate $\log (A/s^{-1}) = 16.5 \pm 1.3$ is applied in order to derive reliable lower and upper limits for E_a from the measured rate constants k_{-3} when there are no accurate experimental activation energies available. Again, either the experimental 2σ error of E_a or that derived from the assumed maximum range of A factors is applied whichever value is smaller. In the following paragraphs, the experimental data for different RO_2NO_2 from this work are presented in the order of decreasing decomposition rate constants k_{-3} at 298 K, i.e., in the order of increasing thermal stability of the corresponding RO_2NO_2.

$C_6H_{11}O_2NO_2$ (Cyclohexyl Peroxynitrate)

Cyclohexyl peroxynitrate was prepared in situ by photolysis of c-$C_6H_{12}/Cl_2/NO_2/O_2/N_2$ mixtures. Its IR spectrum exhibits bands centered at 790 and 1297 cm^{-1} and a double maximum at 1713/1718 cm^{-1}. Thermal decomposition rate constants were determined in 3 experiments at temperatures close to 253 K by following the intensity of the IR band at 1713/1718 cm^{-1} as a function of time. At higher temperatures, thermal decomposition was too fast to be measured, and lower temperatures were not accessible in these experiments. Assuming a preexponential factor of 1.0×10^{16} s^{-1} (see previous section), the Arrhenius expression

$$k_{-3}(C_6H_{11}O_2NO_2) = 1.0 \times 10^{16} \exp[-(87.4 \pm 4.9) \text{ kJ mol}^{-1}/RT] \text{ s}^{-1},\ p = 1000 \text{ mbar},\ M = N_2$$

results. The quoted error limits for the activation energy correspond to the assumed maximum possible range of A ($\log (A/s^{-1}) = 16.0 \pm 1.0$, see previous section). The value of $k_{-3}(C_6H_{11}O_2NO_2)$ at 253 K is about 25% lower as compared to that measured previously for n-hexyl peroxynitrate [9].

$CH_3C(O)CH_2O_2NO_2$ (Acetonyl Peroxynitrate)

$CH_3C(O)CH_2O_2NO_2$ was produced at ppm levels by photolysis of $CH_3C(O)CH_3/Cl_2/O_2/NO_2/N_2$ mixtures in the presence of a large excess of acetone (ca. 0.07 mbar) in order to prevent the reaction of the peroxynitrate with Cl atoms. The principal IR absorption bands of the peroxynitrate are centered at 1731, 1296, and 788 cm^{-1}. Thermal decomposition rate constants were measured at total pressures of 800, 100, and 10 mbar in the temperature range 246–260 K. At these low temperatures, large amounts of N_2O_4 were formed in the course of the reaction whose IR absorption bands interfered with the 1731 and 788 cm^{-1} bands of the peroxynitrate. For this reason, the 1296 cm^{-1} band was selected for the determination of k_{-3}. PAN was detected as a side product by means of the position and time behavior of its absorption bands at 1841 and 1163 cm^{-1}. PAN exhibits an absorption band at 1300 cm^{-1} which is superimposed to the 1296 cm^{-1} band of $CH_3C(O)CH_2O_2NO_2$. However, since PAN is stable at the reaction temperatures and time scales of these experiments, the absorption at 1296 cm^{-1} which remained at long reaction times was assigned to PAN. It was subtracted from all spectra before the first-order loss rate constant was determined, thus, delivering k_{-3}. The temperature and pressure dependence of k_{-3} is shown in Figure 1. The Arrhenius plot of the data

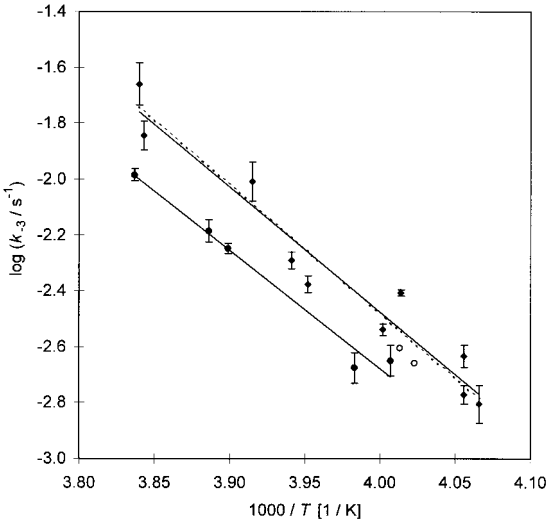

Figure 1 Arrhenius plots for the thermal decomposition rate constant of acetonyl peroxynitrate at total pressures of 800 mbar (full diamonds), 100 mbar (open circles), and 10 mbar (full circles), M = N_2; error limits are 2σ errors of the log (absorbance at 1296 cm^{-1}) = $f(t)$ plots; full lines are least-squares plots of the data points at 800 and 10 mbar, the broken line is the recommended Arrhenius expression for 800 mbar with A fixed at 1.0×10^{16} s^{-1} (see text).

points at 800 mbar shows fairly strong scatter, possibly due to interference by absorption from a side product. The Arrhenius expression derived for 800 mbar is $k_{-3}(CH_3C(O)CH_2O_2NO_2) = 2.6 \times 10^{15}\exp[=(85.6 \pm 15)$ kJ mol$^{-1}/RT]$ s^{-1} (2σ). Fixing the A factor at 1×10^{16} s^{-1} and limiting the range of possible A factors to log (A/s^{-1}) = 16.0 ± 1.0 (see above), the following Arrhenius expression is obtained:

$$k_{-3}(CH_3C(O)CH_2O_2NO_2) = 1.0 \times 10^{16}\exp[-(88.4 \pm 4.9) \text{ kJ mol}^{-1}/RT] \text{ s}^{-1},\ p = 800 \text{ mbar, M} = N_2.$$

The pressure fall-off is only 3% between 1000 and 100 mbar and 12% between 1000 and 10 mbar. Therefore, the pressure dependence of $k_{-3}(CH_3C(O)CH_2O_2NO_2)$ is negligible for atmospheric applications. The observed small fall-off is close to what one would expect for a molecule of this size [5].

$C_6H_5CH_2O_2NO_2$ (Benzyl Peroxynitrate)

Toluene is a major additive of gasoline; typical mass ratios are 8–9 weight % [12]. Emission rates are very high (see, e.g., [13] for emission rates in the U. K.), and mixing ratios in strongly polluted air are up to 80 ppb [14,15]. Degradation of toluene in the atmosphere is initiated predominantly by the addition of OH,

$$OH + C_6H_5CH_3\ (+M) \longrightarrow C_6H_5CH_3 \cdot OH\ (+M) \quad (7a)$$

and by abstraction of an H atom from the side chain,

$$OH + C_6H_5CH_3 \longrightarrow C_6H_5CH_2 + H_2O. \quad (7b)$$

The ratio $k_{7b}/(k_{7a} + k_{7b})$ is about 0.1 [16]. In the photolysis of $C_6H_5CH_3/Cl_2/O_2/NO_2/N_2$ mixtures at temperatures below 260 K both benzyl peroxynitrate and benzoyl peroxynitrate are detected in the IR spectrum. The latter compound is formed as a side product according to the following mechanism:

$$C_6H_5CH_2OO + C_6H_5CH_2OO \text{ (or NO)} \longrightarrow C_6H_5CH_2O + \text{products} \quad (8)$$

$$C_6H_5CH_2O + O_2 \longrightarrow C_6H_5CHO + HO_2 \quad (9)$$

$$C_6H_5CHO + Cl \longrightarrow C_6H_5CO + HCl \quad (10)$$

$$C_6H_5CO + O_2(+M) \longrightarrow C_6H_5C(O)O_2\ (+M) \quad (11)$$

$$C_6H_5C(O)O_2 + NO_2\ (+M) \longrightarrow C_6H_5C(O)O_2NO_2\ (+M) \quad (12)$$

As opposed to OH radicals, Cl atoms almost exclusively abstract an H atom from the side-chain rather than adding to the ring [17]. $C_6H_5C(O)O_2NO_2$ accumulates in the reaction chamber since it is considerably more thermally stable [18–20] than $C_6H_5CH_2O_2NO_2$. The main IR absorption bands of benzyl peroxynitrate are at 1720, 1299, 1249, 793, and 741 cm^{-1}. Since the benzoyl peroxynitrate band at 1741 cm^{-1} and the benzyl peroxynitrate band at 1720 cm^{-1} do not interfere, the first-order decay of the 1720 cm^{-1} band can be evaluated between 248 and 259 K. A least-squares fit of the data with A fixed at 1.0×10^{16} s^{-1} (see Fig. 2) leads to

$$k_{-3}(C_6H_5CH_2O_2NO_2) = 1.0 \times 10^{16}\exp[-(89.8 \pm 5.6) \text{ kJ mol}^{-1}/RT) \text{ s}^{-1},\ p = 1000 \text{ mbar, M} = N_2.$$

$CH_2IO_2NO_2$ (Iodomethyl Peroxynitrate)

The possible role of iodine in both the troposphere [21] and the stratosphere [22] has been thoroughly discussed in the literature. Recently, it has been suggested that iodine may be of importance for the ozone loss in the lower stratosphere [22]. Methyl iodide is believed to be the major iodine compound in the atmosphere; its annual emission rate has been estimated to be 1.5 Tg/yr [22]. Although the reaction of CH_3I with OH radicals can lead to $CH_2IO_2NO_2$, the predominant fate

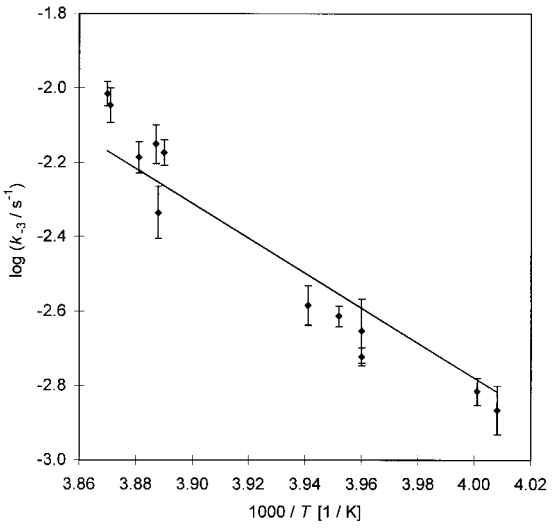

Figure 2 Arrhenius plot for the thermal decomposition rate constant of benzyl peroxynitrate at a total pressure of 1000 mbar (M = N_2); the full line is the recommended Arrhenius expression with A fixed at 1.0×10^{16} s^{-1} (see text). Error limits of the data points are 2σ errors of the first-order plots of log absorbance = $f(t)$; the cause for the apparently steeper increase of the data points at high temperatures is not known.

of CH_3I in the troposphere is ejection of the I atom by photolysis [22], thus, preventing the formation of CH_2I and $CH_2IO_2NO_2$. However, it has also been suggested that diiodomethane is emitted from the oceans with an emission rate comparable to that of CH_3I [23], and the photolysis of CH_2I_2 leads to CH_2I radicals [24] which can form $CH_2IO_2NO_2$ in the troposphere.

$CH_2IO_2NO_2$ (iodomethyl peroxynitrate) was prepared by the photolysis of $CH_2I_2/O_2/NO_2/N_2$ mixtures at $\lambda \geq 300$ nm in the temperature range 254–263 K. There was no experimental evidence for the reaction $CH_2I + O_2 \rightarrow CH_2OO + I$ which was proposed by Schmitt and Comes [24] in order to explain the observed reduced reformation of CH_2I_2 in the photolysis of CH_2I_2 when O_2 is present [25].

In three experiments between 253 and 256 K, first-order decay rate constants were determined by monitoring the absorbance of the IR band at 989 cm^{-1} as a function of time. The following Arrhenius expression can be derived at 1000 mbar, assuming log (A/s^{-1}) = 16.0 ± 1.0 for the preexponental factor:

$$k_{-3}(CH_2IO_2NO_2) = 1.0 \times 10^{16}\exp[-(91.8 \pm 4.9)\ \text{kJ mol}^{-1}/RT]\ s^{-1},\ p = 1000\ \text{mbar},\ M = N_2.$$

$CH_3C(O)OC(H)(CH_3)O_2NO_2$ (Acetoxyethyl Peroxynitrate)

The thermal decomposition of acetoxyethyl peroxynitrate was investigated in order to examine the effect of substituting an H atom in (substituted) methyl peroxynitrates by the R′C(O)O group. This type of peroxynitrate is formed by H atom abstraction from carboxylic acid esters. In the present work, $CH_3C(O)OC(H)(CH_3)O_2NO_2$ was prepared in situ by photolysis of $CH_3C(O)OCH_2CH_3/Cl_2/O_2/NO_2/N_2$ mixtures at $\lambda \geq 300$ nm in the temperature range 259–277 K. The precursor molecule can be attacked by Cl atoms at three different sites, leading to different peroxynitrates:

$$CH_3C(O)OCH_2CH_3 + Cl \longrightarrow CH_2C(O)OCH_2CH_3 + HCl \longrightarrow \cdots \longrightarrow CH_3CH_2OC(O)CH_2O_2NO_2 \quad (14a)$$

$$CH_3C(O)OCH_2CH_3 + Cl \longrightarrow CH_3C(O)OCH_2CH_2 + HCl \longrightarrow \cdots \longrightarrow CH_3C(O)OCH_2CH_2O_2NO_2 \quad (14b)$$

$$CH_3C(O)OCH_2CH_3 + Cl \longrightarrow CH_3C(O)OC(H)CH_3 + HCl \longrightarrow \cdots \longrightarrow CH_3C(O)OC(H)(CH_3)O_2NO_2 \quad (14c)$$

After switching off the lights and adding excess NO, the typical peroxynitrate bands disappeared with 3 distinctly different time constants. The shortest-lived absorption was assigned to $CH_3CH_2OC(O)CH_2O_2NO_2$ and $CH_3C(O)OCH_2CH_2O_2NO_2$ which derive from acetonyl peroxynitrate and ethyl peroxynitrate, respectively, by substituting a ligand of the C atom which is in β position to the peroxy group. Thus, these peroxynitrates are expected to be as short-lived as $CH_3C(O)CH_2O_2NO_2$ and $CH_3CH_2O_2NO_2$ ($1/k_{-3}$ = several seconds at 298 K, 1 bar). The longest-lived peroxynitrate in this reaction system was identified as PAN both by its IR absorption bands and its decomposition rate. The formation of PAN can easily be rationalized by the unimolecular decomposition of the radical which is produced in channel (14c):

$$CH_3C(O)OC(H)CH_3\ (+M) \longrightarrow CH_3CO + CH_3CHO\ (+M) \quad (15)$$

$$CH_3CO + O_2 + NO_2\ (+M) \longrightarrow CH_3C(O)O_2NO_2\ (\text{PAN})\ (+M) \quad (16)$$

Peroxynitrate bands of intermediate lifetime appearing at 1727, 1299, 1225, 1105, and 793 cm^{-1} can then unambiguously be assigned to $CH_3C(O)OC(H)(CH_3)O_2NO_2$

which is formed from the $CH_3C(O)OC(H)CH_3$ radical (reaction (14c)), in competition to the unimolecular decomposition channel (reaction (15)).

The product carbonyl bands between 1800 and 1850 cm^{-1} are superimposed by strong bands of $CH_3C(O)OCH_2CH_3$ and cannot be used for product identification. When the absorption cross sections of the typical peroxynitrate bands at 1300 cm^{-1} are assumed to be the same for all of these peroxynitrates of different lifetimes, the following fractions of the individual peroxynitrates can be deduced from the time behavior of the IR absorption at 1300 cm^{-1}:

$CH_3CH_2OC(O)CH_2O_2NO_2$
$+ CH_3C(O)OCH_2CH_2O_2NO_2$:
10–20% (short lifetime)

$CH_3C(O)OC(H)(CH_3)O_2NO_2$:
40–70% (intermed. lifetime)

$CH_3C(O)O_2NO_2$: 20–40% (long lifetime),

the acetoxyethyl peroxynitrate, thus, being the major peroxynitrate. These figures correspond to 10–20% H atom abstraction from the primary C atoms in the precursor compound acetic acid ethyl ester and 80–90% abstraction from the secondary C atom.

For the rate constant determinations, the time behaviors of the IR bands of $CH_3C(O)OC(H)(CH_3)O_2NO_2$ at 1103 and 1223 cm^{-1} were evaluated as a function of time. The first-order decay rate constants obtained from both bands are shown in Figure 3. They were averaged and resulted in the following Arrhenius expression:

$$k_{-3}(CH_3C(O)OC(H)(CH_3)O_2NO_2) = 1.0 \times 10^{16}\exp[-(94.9 \pm 5.1)\ \text{kJ mol}^{-1}/RT]\ \text{s}^{-1}\ (2\sigma),\quad p = 1000\ \text{mbar},\ M = N_2.$$

In this expression, the preexponential factor of k_{-3} was assumed to be represented by $\log (A/s^{-1}) = 16.0 \pm 1.0$, and the error of the activation energy was chosen so that it corresponds to the uncertainty of the A factor.

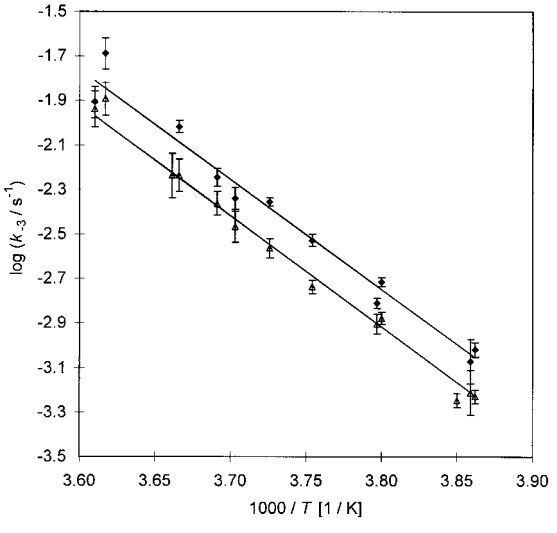

Figure 3 Arrhenius plots for the thermal decomposition rate constant of acetoxyethyl peroxynitrate at a total pressure of 1000 mbar ($M = N_2$) as derived from the 1103 cm^{-1} (full diamonds) and 1223 cm^{-1} (open triangles) IR bands; the A factor is fixed at 1.0×10^{16} s^{-1} (see text).

$C_6H_5OCH_2O_2NO_2$ (Phenoxymethyl Peroxynitrate)

Phenoxymethyl peroxynitrate has a structure similar to acetoxyethyl peroxynitrate (i.e., $R'OC(H)_n(R)_{2-n}O_2NO_2$). For this reason, its decomposition rate constants are expected to be close to those of $CH_3C(O)OC(H)(CH_3)O_2NO_2$. In order to check this presumption, phenoxymethyl peroxynitrate was prepared in situ from $C_6H_5OCH_3/Cl_2/O_2/NO_2/N_2$ mixtures by photolysis at $\lambda \geq 300$ nm in the temperature range 267–276 K. In analogy to toluene, the precursor is expected to be attacked by Cl atoms only at the methyl group and not at the aromatic ring. The IR absorption bands of this peroxynitrate appear at 1727, 1304, 1087, 942, and 796 cm^{-1}. The time behaviors of the 1727 and 942 cm^{-1} bands were separately evaluated, leading to nearly identical rate constants (within 5%). The rate constants deduced from these bands for 6 experiments are shown in Figure 4, resulting in the Arrhenius expression

$$k_{-3}(C_6H_5OCH_2O_2NO_2) = 1.0 \times 10^{16}\exp[-(95.0 \pm 5.2)\ \text{kJ mol}^{-1}/RT]\ \text{s}^{-1}\ (2\sigma),\quad p = 1000\ \text{mbar},\ M = N_2.$$

Again, the preexponential factor is assumed to be represented by $\log (A/s^{-1}) = 16.0 \pm 1.0$, and the error of the activation energy is chosen so that it accounts for the uncertainty of the A factor. As expected, the thermal decomposition rate constant of this peroxynitrate is nearly identical to that of $CH_3C(O)OC(H)(CH_3)O_2NO_2$.

$(CH_3)_2NC(O)O_2NO_2$ (*N,N*-Dimethylaminoformyl Peroxynitrate)

N,N-Dimethylaminoformyl peroxynitrate was prepared in situ by photolysis of $(CH_3)_2NC(O)H/Cl_2/O_2/$

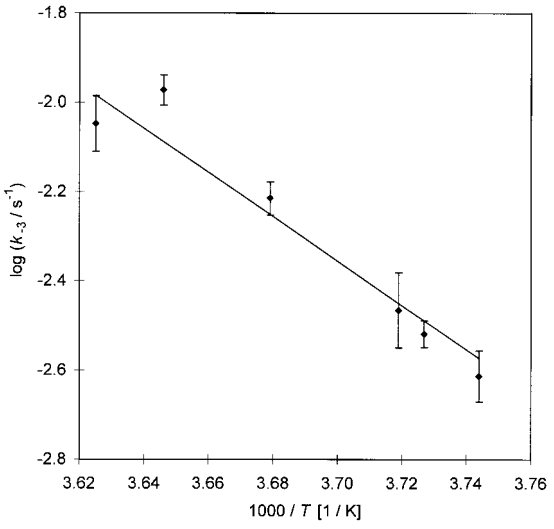

Figure 4 Arrhenius plot for the thermal decomposition rate constant of phenoxymethyl peroxynitrate at a total pressure of 1000 mbar (M = N_2); the *A* factor is fixed at 1.0×10^{16} s^{-1} (see text).

NO_2/N_2 mixtures at $\lambda \geq 300$ nm in the temperature range 267–276 K. Due to the considerably lower bond energy of the H atom connected to the carbonyl C atom as compared to the H atoms of the methyl groups, the desired peroxynitrate was selectively formed. In addition, the peroxynitrate deriving from the attack of the methyl groups should be thermally much less stable. $(CH_3)_2NC(O)O_2NO_2$, on the other hand, is expected to be long-lived due to its similarity to PAN. The observed IR bands are centered at 1811, 1740, 1389, 1300, 1274, 1135, 1048, 978, and 796 cm^{-1}; the 796 cm^{-1} band was used for the evaluation of the decay rates. From 10 experiments in the temperature range 301–315 K the following Arrhenius expression was derived (see Fig. 5):

$$k_{-3}((CH_3)_2NC(O)O_2NO_2) = 4.3 \times 10^{16} \exp[-(111.5 \pm 5.8)\ \text{kJ mol}^{-1}/RT]\ \text{s}^{-1}\ (2\sigma),\quad p = 1000\ \text{mbar, M} = N_2.$$

The given *A* factor is close to the value assumed to be typical for substituted formyl peroxynitrates (i.e., log $(A/s^{-1}) = 16.5 \pm 1.3$, see above). The 2σ error of the activation energy as derived from the Arrhenius plot is smaller than the uncertainty of E_a arising from the stated uncertainty of the preexponential factor *A*.

$C_6H_5OC(O)O_2NO_2$ (Phenoxyformyl Peroxynitrate)

Phenoxyformyl peroxynitrate was prepared in situ by photolysis of $C_6H_5OC(O)H/Cl_2/O_2/NO_2/N_2$ mixtures at $\lambda \geq 300$ nm in the temperature range 302–316 K. Prominent IR absorption bands appeared at 1844, 1746, 1310, 1216, 982, and 798 cm^{-1}. For the kinetic experiments, the band centered at 1216 cm^{-1} was evaluated. The experiments indicated that there was an unidentified loss process for $C_6H_5OC(O)O_2$ radicals, in addition to reactions (3) and (6), which could be suppressed by the addition of higher amounts of NO_2. Thus the wall loss rate constant k_w of $C_6H_5OC(O)O_2NO_2$ was determined in 4 separate experiments in the presence of excess NO_2 (50 ppm). k_w was in the range $(2-5) \times 10^{-4}$ s^{-1}. The lower and upper limits of k_w were assumed to be 0 and 5×10^{-4} s^{-1}, respectively, and a mean value of 2.5×10^{-4} s^{-1} was applied to correct the effective first-order decay rate constants for wall loss. 10 experiments were performed at $p_{NO_2}/p_{tot} \ll 50$ ppm and $[NO] \gg [NO_2]$ in order to determine k_{-3}. The following Arrhenius expression was derived (see Fig. 6):

$$k_{-3}(C_6H_5OC(O)O_2NO_2) = 3 \times 10^{16} \exp[-(112.7 \pm 7.7)\ \text{kJ mol}^{-1}/RT]\ \text{s}^{-1}\ (2\sigma),\quad p = 1000\ \text{mbar, M} = N_2.$$

For the *A* factor, the value 3×10^{16} s^{-1} was applied which is typical for acyl peroxynitrates. The stated er-

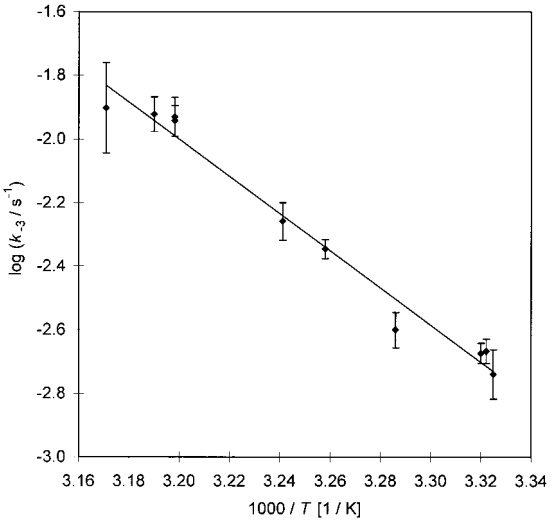

Figure 5 Arrhenius plot for the thermal decomposition rate constant of *N,N*-dimethylaminoformyl peroxynitrate at a total pressure of 1000 mbar (M = N_2); the full line is the least-squares plot of the data points.

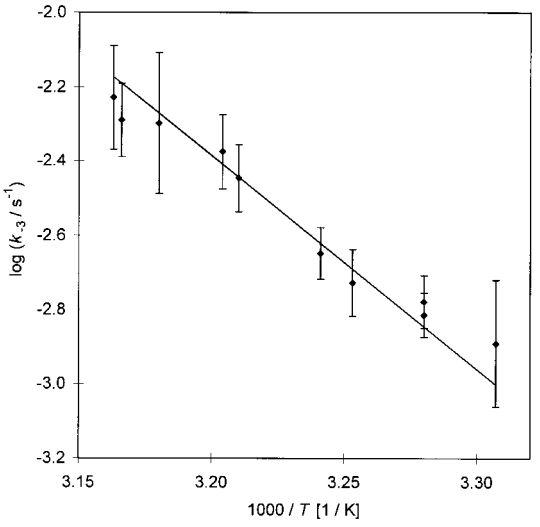

Figure 6 Arrhenius plot for the thermal decomposition rate constant of phenoxyformyl peroxynitrate at a total pressure of 1000 mbar (M = N_2); the A factor is fixed at 3×10^{16} s^{-1} (see text).

ror of the activation energy corresponds to a possible range of A factors between 1.5×10^{15} and 6×10^{17} s^{-1} (see earlier section).

$C_2H_5C(O)O_2NO_2$ (Propionyl Peroxynitrate)

Propionyl peroxynitrate is one of the ubiquiteous peroxynitrates accompanying PAN at levels between 5 and 30% of the mixing ratios of PAN (e.g., [26,27]). Propionyl peroxynitrate was prepared by two methods: (1) for the kinetic experiments, $CH_3CH_2CHO/Cl_2/O_2/NO_2/N_2$ mixtures were photolyzed in situ with light of $\lambda \geq 300$ nm at temperatures between 301 and 320 K and total pressures between 10 and 1000 mbar (M = N_2) and (2) for the preparation of samples which were supposed to be free of PAN and chlorine containing compounds, peroxypropionic acid was nitrated by HNO_3 in *n*-tridecane solution as described by Nielsen et al. [28]. Peroxypropionic acid was synthesized by the method of D'Ans and Frey [29].

The IR spectrum of propionyl peroxynitrate shows absorption bands centered at 2996.4, 2960.5, 1833.7, 1738.5, 1467.2, 1432.4, 1347.3, 1299.7, 1156.2, 1097, 1042.9, 990.1, 963.1, 920.6, 851.1, 793.1, and 582 cm^{-1}, and is in good agreement with the spectrum presented by Gaffney et al. [30]. From the progress of the IR absorptions at 1738.5 and 1042.9 cm^{-1} with time, first-order rate constants were separately determined and averaged (details can be found in ref. [31]). The data obtained at different temperatures and total pressures are summarized in Table I and Figure 7. In agreement with unimolecular rate theories, both the absolute rate constants and the activation energies decrease with decreasing total pressure. For atmospheric applications, the Arrhenius expression at 1000 mbar (see Table I) can be used. The pressure dependence of k_{-3} can be described by the fall-off expression

Table I Arrhenius Parameters for the Thermal Decomposition of Propionyl Peroxynitrate (M = N_2)

p_{tot} [mbar]	T [K]	A [s^{-1}]	E_a [kJ mol^{-1}]
1013	291–320	7.2×10^{16}	115.9 ± 2.2 (2σ)
103	300–318	1.5×10^{16}	112.1 ± 4.7 (2σ)
11.5	298–318	1.5×10^{15}	106.9 ± 3.3 (2σ)

$$\log(k/k_\infty) = \log\{(k_0/k_\infty)/(1 + k_0/k_\infty)\} + \log(F_c) \times \{1 + [\log(k_0/k_\infty)/N_c]^2\}^{-1}, \quad \text{(II)}$$
$$N_c = 0.75 - 1.27 \times \log(F_c),$$

as suggested by Troe [32], with the following parameters:

$$k_0(T) = [N_2] \times 1.7 \times 10^{-3}\exp[-93.8 \text{ kJ mol}^{-1}/RT] \text{ cm}^3\text{molecule}^{-1}\text{s}^{-1}$$

$$k_\infty(T) = 8.3 \times 10^{16}\exp[-(115.9 \pm 2.2) \text{ kJ mol}^{-1}/RT] \text{ s}^{-1} (2\sigma)$$

$$F_c = 0.36$$

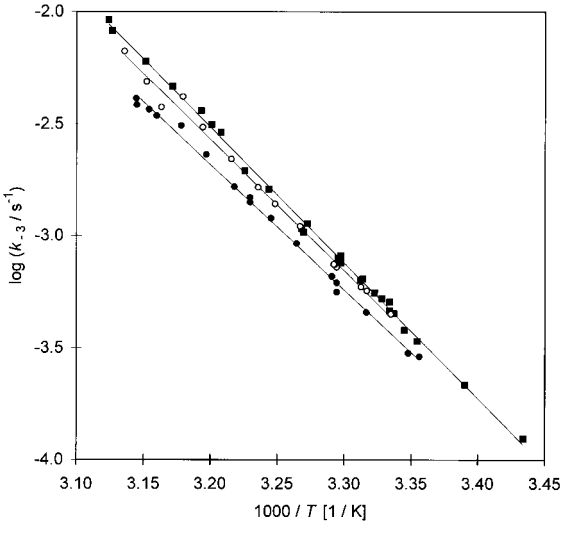

Figure 7 Arrhenius plots for the thermal decomposition rate constant of propionyl peroxynitrate at total pressures of 1000 mbar (full squares), 100 mbar (open circles), and 10 mbar (full circles), M = N_2.

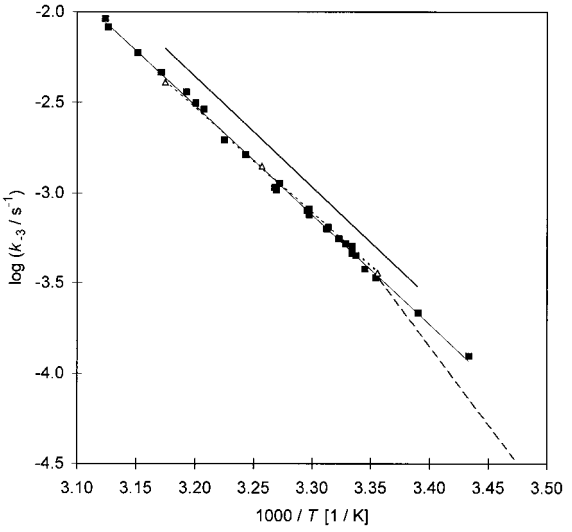

Figure 8 Comparison of the thermal decomposition rate constants of propionyl peroxynitrate at atmospheric pressure with literature data—heavy full line: Schurath and Wipprecht [35]; triangles and dotted line: Mineshos and Glavas [37]; broken line: Grosjean et al. [36]; full squares and full line: this work.

F_c was calculated using the available experimental frequencies of fundamentals of $C_2H_5C(O)O_2NO_2$ and MNDO calculated values for the (essentially low) unknown frequencies [33]. In Figure 8, the kinetic data at 1000 mbar from this work are compared with literature data of Schurath and Wipprecht [35], Grosjean et al. [36], and Mineshos and Glavas [37]. Compared to the present work, the data of Wipprecht and Schurath show nearly the same activation energy (lower by 0.7 kJ mol^{-1}) but rate constants which are consistently higher by 30%. Contrary to this, the rate constants of Grosjean et al. [36] are identical to those of the present work at room temperature but show a stronger temperature dependence. However, in the common experimental temperature range the rate constants from different groups agree within the combined error limits. The rate constants measured by Mineshos and Glavas [37] at 298, 307, and 315 K are in excellent agreement with the present rate constants deduced from the Arrhenius expression for 1000 mbar.

DISCUSSION

In Table II, the present and previous data from this laboratory on the thermal decomposition of peroxynitrates are summarized. The following conclusions can be drawn from Table II: (i) Thermal lifetimes of peroxynitrates depend on temperature and pressure. However, the existing pressure dependent data show that for most peroxynitrates Arrhenius parameters measured at or calculated for 1 bar apply for the total pressure range of the lower troposphere ($>$ 400 mbar) within 10%; (ii) Thermal lifetimes of peroxynitrates depend on the chemical nature of R. With respect to their lifetimes at identical reaction conditions, essentially three classes of peroxynitrates can be differentiated: (I) Stable peroxynitrates with thermal lifetimes $\geq 10^3$ s at 298 K, 1 bar. All peroxynitrates of this group have a carbonyl group next to the peroxy group in common, i.e., their structure is $R'C(O)O_2NO_2$. (II) Unstable peroxynitrates with thermal lifetimes $\leq$ 1 s at 298 K, 1 bar. All peroxynitrates of the structure $RC(R')(R'')O_2NO_2$ belong to this group provided that neither of the groups R, R′, and R″ is a strongly electron drawing substituent. These peroxynitrates are much too unstable to accumulate in the lower troposphere. However, they can be formed in laboratory experiments which simulate atmospheric degradation processes, e.g., of biogenic and aromatic hydrocarbons, at relatively high NO_X levels. In special cases, when the atmospheric source strength of these peroxynitrates is high, as is the case for methyl peroxynitrate, they can accumulate in the upper troposphere to significant levels. Although many organic substances R—H have recently been detected in the lower stratosphere [38], the source strength of most of the corresponding peroxynitrates RO_2NO_2 is probably too small to make them important reservoirs of NO_X. (III) Peroxynitrates of intermediate stability with thermal lifetimes between 1 and 1000 s at 298 K, 1 bar. This group includes HO_2NO_2 and peroxynitrates of the structure $RC(R')(R'')O_2NO_2$ where R and/or R′ and/or R″ are strongly electron drawing substituents (e.g., alkoxy, halogen); (iii) Different lifetimes of RO_2NO_2 are mainly the result of different bond energies (activation energies for thermal decomposition between 85 and 120 kJ mol^{-1}). In addition, there appears to be a slight systematic increase of the Arrhenius preexponential factor with the activation energy; and (iv) Thermal lifetimes of peroxynitrates of the structure $R'CH_2O_2NO_2$ are very similar since the electron withdrawing effect of the group R′ has only a small influence on the OO—N bond energy due to the screening effect of the CH_2 group. This is particularly obvious in the case of acetonyl peroxynitrate which is, contrary to PAN, very short-lived. Peroxynitrates of the structure $R'CH_2O_2NO_2$ are thermally less stable than PAN by more than 3 orders of magnitude.

Summarizing, the different thermal stabilities of peroxynitrates RO_2NO_2 with different R can be qualitatively understood by the inductive effect of R. Based on the results summarized in Table II, in par-

Table II Kinetic Parameters for the Thermal Decomposition of Peroxynitrates (RO_2NO_2 (+M) → RO_2 + NO_2 (+M))[a]

R	$k_{298\ K,\ 1\ bar}$, M = N_2[b,c] [s^{-1}]	$E_{a,\infty}$ [kJ mol^{-1}]	A_∞ [10^{16} s^{-1}]	F_c	$A_0/[N_2]$ [cm^3molecule$^{-1}s^{-1}$]	$E_{a,0}$ [kJ mol^{-1}]	$E_{a,1\ bar}$[b] [kJ mol^{-1}]	$A_{1\ bar}$[f] [10^{16} s^{-1}]	$k_\infty/k_{1\ bar}$[d] (fall-off)	Ref.
C_6H_{11}	4.8						87.4 ± 4.8[e]	1[f]		this work
C_2H_5	3.7[g]	86.7 ± 4.0	0.76	0.4	3.6×10^{-4}	77.7	86.2 ± 4.0[g,b]	0.47[g]	1.31	[9]
$CH_3C(O)CH_2$	3.2[g]	87.6 ± 10	0.76	0.3			88.4 ± 4.8[e]	1[f]		this work
CF_2ClCH_2	2.3						90.9 ± 5.9[e]	2[f]		[39]
$CFCl_2CH_2$	2.1						91.2 ± 5.3[e]	2[f]		[39]
$C_6H_5CH_2$	1.8						89.8 ± 4.8[e]	1[f]		this work
CH_3	1.64	87.8 ± 5.9	1.1	0.4	9.0×10^{-5}	80.6	83.8 ± 5.9	0.080	2.53	[9]
$HOCH_2$	1.0[i]						85.3[f]	0.09[j]		[40]
CH_2I	0.81						91.8 ± 4.9[e]	1[f]		this work
CH_3OCH_2	0.45	94.1 ± 6.0	1.76	0.4	5.8×10^{-3}	85.5	93.5 ± 5.4[h]	1.1	1.15	[41]
CH_2Cl	0.26[g]	93.5 ± 2.9	1.05	0.36	6.6×10^{-4}	85.9	91.7 ± 2.9[g,h]	0.31[g]	1.40	[7]
$CH_3C(O)OCH(CH_3)$	0.23						94.9 ± 5.1[e]	1[f]		this work
$C_6H_5OCH_2$	0.22						95.0 ± 5.2[e]	1[f]		this work
CCl_3	0.19[g]	98.3 ± 1.4	4.8	0.22	6.3×10^{-3}	85.1	96.8 ± 1.4[g,h]	1.8[g]	1.18	[10]
H	0.083	92.9 ± 7.2	0.57	0.5	4.0×10^{-5}	88.5 ± 2.2[h]	89.2 ± 2.2[h]	0.036	3.93	[7]
CCl_2F	0.066[g]	101.8 ± 1.8	6.6	0.28	1.01×10^{-2}	90.3	100.3 ± 1.8[g,h]	2.5[g]	1.18	[10]
$CClF_2$	0.040[g]	99.7 ± 1.7	1.6	0.30	1.8×10^{-3}	87.3	98.7 ± 1.8[g,h]	0.8[g]	1.17	[10]
$(CH_3)_2NC(O)$	0.0012						111.5 ± 5.8[h]	4.3		this work
$CH_3OC(O)$	0.00084	108.1 ± 5.0	0.88	0.3	4.7×10^{-3}	94.6	107.0 ± 4.5[h]	0.48	1.10	[41]
$C_6H_5OC(O)$	0.00053						112.7 ± 7.7[e]	3[f]		this work
$CH_3C(O)$	0.00041[g]	113.3 ± 2.5	3.9	0.3	5.5×10^{-3}	100.3	112.9 ± 1.9[g,h]	2.5[g]	1.15	[42,43]
$C_2H_5C(O)$	0.00035	119.2 ± 4.3	36	0.3	4.6×10^{-2}	107.1	115.9 ± 2.2[h]	7.2	1.17	this work
$C_6H_5C(O)$	0.00031	117.0 ± 3.8	11.3	0.25	3.4×10^{-2}	92.6	116.4 ± 3.8[h]	7.9	1.05	this work
ClC(O)	0.00017[g]	116.7 ± 3.2	7.1	0.3	6.9×10^{-3}	105.6	115.1 ± 3.2[g,h]	2.6[g]	1.21	[44]
$CCl_3C(O)$	0.00012[g]	121.6 ± 6.2	32	0.12	4.0×10^{-1}	100.0	120.6 ± 5.2[g,h]	16[g]	1.08	[39]
$CFCl_2C(O)$	0.00012						118.0 ± 5.2[e]	6[f]		[39]
$CF_2ClC(O)$	0.00010						118.6 ± 5.2[e]	6[f]		[39]
$CF_3C(O)$	0.000080	120.1 ± 5.5	11	0.2	4.3×10^{-2}	102.7	119 ± 5.0[e]	6[f]	1.10	[39]

[a]Table includes only data from this laboratory; work from other research groups is discussed in the original articles cited in the last column.

[b]The experiments performed at 1 bar total pressure unless otherwise noted.

[c]When the experimental temperature range does not include 298 K, the given value is calculated from E_a and A in columns 8 and 9.

[d]Calculated from k_0 and k_∞ using the expression $\log(k/k_\infty) = \log[k_\infty/(1 + k_0/k_\infty)] + \log(F_c) \times \{[1 + \log(k_0/k_\infty)]^2\}^{-1}$ (Troe [32]).

[e]Value estimated from measured k value and assumed A factor, see original article.

[f]Assumed value, see original article.

[g]Measured at 800 mbar total pressure.

[h]2 σ error.

[i]Measured at 533 mbar total pressure.

[j]Value estimated from measured k value and assumed E_a, see original article.

ticular the absolute rate constants at 298 K, reliable estimates of the thermal lifetimes can be achieved for those RO_2NO_2 which have not been subject to experimental measurements. This is useful for the interpretation of product IR spectra in laboratory work on the degradation of hydrocarbons since, in the presence of O_2 and NO_2, one has always to be aware of the formation of peroxynitrates.

To put the qualitative estimates of the thermal stabilities of unknown peroxynitrates based on Table II on a more objective basis, a new approach was pursued to correlate thermal rate constants k_{-3} with easily available n.m.r. data. The basic idea is that both the ^{13}C n.m.r. shift of the carbon atom connected to the peroxy group in a certain peroxynitrate and its OO—NO_2 bond energy depend on the electron density in the vicinity of this carbon atom. Likewise, Parlar et al. [45] showed that there is a strong correlation between the rate constants for the reaction of OH radicals with alkanes, alcohols, ethers, and esters, and the ^{13}C n.m.r. shifts of the carbon atoms connected to those H atoms which are abstracted by OH. Unfortunately, at the time when these correlations were elucidated for the thermal decomposition rate constants of RO_2NO_2 [6], virtually no n.m.r. data of peroxynitrates were available. For this reason, a procedure was

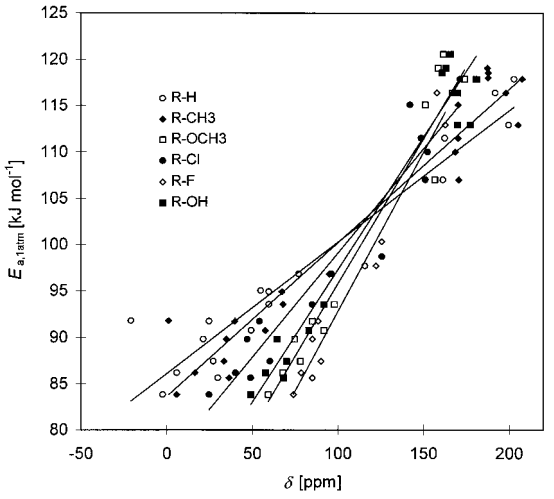

Figure 9 Correlations between experimental activation energies of thermal decomposition rate constants of RO_2NO_2 and the ^{13}C n.m.r. shifts of the carbon atom connected to X in compounds RX. (The two data points at $E_a \approx 92$ kJ mol^{-1} and $\delta \leq 0$, both being strongly off the least-square lines, belong to R = CH_2I, see text.).

initially chosen which is described in the following section.

Application of the ^{13}C n.m.r. Shifts in Compounds RX (X = H, CH_3, OH, OCH_3, Cl, or F)

Due to the lack of experimental data, the kinetic parameters of reaction (−3) were not correlated to ^{13}C n.m.r. shifts in the peroxynitrates RO_2NO_2 but to those in a series of the related compounds RX for a common X. The groups X (X = H, CH_3, OH, OCH_3, Cl, or F) were selected such that a set of ^{13}C n.m.r. data of RX as complete as possible was available for the R of interest. These correlations are shown in Figure 9. From the least-squares fits to the data points for individual X, the following relationships $E_a(\delta) = a_X \times \delta_X + b_X$ were derived:

$$E_a(k_{-3}, 1\ \text{bar})/\text{kJ mol}^{-1} = 0.1534 \times \delta_H/\text{ppm} + 85.03 \quad \text{(IIIa)}$$

$$E_a(k_{-3}, 1\ \text{bar})/\text{kJ mol}^{-1} = 0.1709 \times \delta_{CH_3}/\text{ppm} + 82.53 \quad \text{(IIIb)}$$

$$E_a(k_{-3}, 1\ \text{bar})/\text{kJ mol}^{-1} = 0.2771 \times \delta_{OH}/\text{ppm} + 69.30 \quad \text{(IIIc)}$$

$$E_a(k_{-3}, 1\ \text{bar})/\text{kJ mol}^{-1} = 0.3075 \times \delta_{OCH_3}/\text{ppm} + 65.16 \quad \text{(IIId)}$$

$$E_a(k_{-3}, 1\ \text{bar})/\text{kJ mol}^{-1} = 0.2265 \times \delta_{Cl}/\text{ppm} + 76.53 \quad \text{(IIIe)}$$

$$E_a(k_{-3}, 1\ \text{bar})/\text{kJ mol}^{-1} = 0.3580 \times \delta_F/\text{ppm} + 57.05 \quad \text{(IIIf)}$$

where, e.g., the δ_H values are the ^{13}C n.m.r. shifts in compounds RH for different R, and $E_a(k_{-3}, 1\ \text{bar})$ is the activation energy of the thermal decomposition rate constant of the corresponding peroxynitrate RO_2NO_2. The coefficients a_X and b_X for different X are collected in Table III. By looking up the ^{13}C n.m.r. shift in, for example, CF_3H (R = CH_3, X = H), the activation energy for the thermal decomposition of $CF_3O_2NO_2$ can easily be estimated by application of eq. (IIIa). The agreement of the calculated activation energies with the experimental values can be improved by averaging the activation energies calculated for the same peroxynitrate (i.e., the same R) from eq. (III) for different X. The ^{13}C n.m.r. shift data were taken from Bremser et al. [46,47].

In order to be able to predict rate constants by this method, correlations between preexponential factors and n.m.r. shifts are also needed. Since the experimental values for preexponential factors were strongly scattered, the temperatures T^* at which the experimental rate constants k^* are equal to 3×10^{-3} s^{-1} were correlated with the n.m.r. shifts. The reason for employing this procedure is that the rate constants could be measured quite accurately whereas the determination of the preexponential and exponential terms was subject to larger errors. The value 3×10^{-3} s^{-1} was chosen because it corresponds to the middle of the experimentally accessible range of k values (10^{-4} – 10^{-1} s^{-1}) where the measured rate constants were the

Table III Parameters Needed to Calculate E_a from Eq. (III) and k_{-3} from Eq. (VI)

X =	H	CH_3	OH	OCH_3	Cl	F
a_X [kJ mol^{-1} ppm^{-1}]	0.1420	0.1653	0.2848	0.3116	0.2243	0.3432
b_X [kJ mol^{-1}]	86.04	83.67	68.51	64.60	76.63	58.47
c_X [K ppm^{-1}]	0.3178	0.3742	0.6121	0.6869	0.5043	0.7476
d_X [K]	248.52	243.05	211.36	201.73	228.3	189.65

most accurate. The correlations of T^* as a function of δ were satisfactory and provided the coefficients c_X and d_X:

$$T^* = c_X \times \delta_X + d_X \quad \text{(IV)}$$

The coefficients c_X and d_X for different X are included in Table III [47]. Using eq. (V),

$$\begin{aligned} k^* &= A \times \exp(-E_a/RT^*) \longrightarrow \\ A &= k^* \times \exp(E_a/RT^*) \\ &= k^* \times \exp[(a_X\delta_X + b_X)/RT^*], \end{aligned} \quad \text{(V)}$$

the A factors can be expressed as a function of δ. Combining the expressions for $A(\delta)$ and $E_a(\delta)$, the following modified Arrhenius expression results:

$$\begin{aligned} k_{-3} = 3 &\times 10^{-3} \times \exp\{(a_X\delta_X + b_X)/[\mathrm{Rx}(c_X\delta_X + d_X)]\} \\ &\times \exp\{-(a_X\delta_X + b_X)/RT\}\ \mathrm{s}^{-1}, \end{aligned} \quad \text{(VI)}$$

where a_X, b_X, c_X, and d_X are the intercepts and slopes of the correlations of E_a and T^* as a function of δ. The meaning of the individual terms in eq. (VI) becomes clearer by comparison with eq. (VII),

$$\begin{aligned} k &= A \times \exp(-E_a/RT) \\ &= k^* \times \exp(E_a/RT^*) \times \exp(-E_a/RT). \end{aligned} \quad \text{(VII)}$$

The procedure for predicting thermal decomposition rate constants of a certain peroxynitrate RO_2NO_2 is the following: (i) Look up the ^{13}C n.m.r. shifts δ in compounds RX with X = H and/or CH_3, OH, OCH_3, Cl, and F; (ii) For a certain X, calculate k_{-3} by inserting the δ value and the appropriate values for the parameters a_X, b_X, c_X, and d_X from Table III into eq. (VI); and (iii) If you find δ values for RX with different X, calculate the corresponding k_{-3} separately, and average the k_{-3} values in order to reduce the error limits.

If this procedure is applied to all those examples included in Table II where ^{13}C data of RX are available, the k values calculated for the mean temperature of the experiments deviate from the experimental value by less than a factor of 6 and typically by less than a factor of 3 (in the average by a factor of 2.6, see Table IV). There is one exception: the calculated value for $CH_2IO_2NO_2$ is larger by a factor of 25 than the experimental value. This difference is probably related to the well known 'heavy atom effect" in ^{13}C n.m.r. spectroscopy which has been attributed to the strong diamagnetic shielding produced by the large number of electrons in heavy substituents in α position, in particular of iodine [48].

The average deviation by a factor of 2.6 between the calculated and experimental k_{-3} values seems to be high; however, if the rate constants are estimated by other methods, e.g., using HKRRM theory, one should be aware of the need to estimate both the bond energy and uncertain vibrational frequencies (for the A factor). The average error of the calculated k_{-3} values of a factor of 2.6 corresponds to an error of the activation energy of only 2.4 kJ mol^{-1} at 298 K. For $CH_3O_2NO_2$, a major part of the difference between the calculated and the experimental k_{-3} value is due to the larger fall-off of k_{-3} at 1 bar ($k_\infty/k_{1\mathrm{bar}} \approx 2.5$) as compared to the fall-off of most of the other RO_2 NO_2 on which the correlation is based ($k_\infty/k_{1\mathrm{bar}} \approx 1.2 \pm 0.1$, see Table II for comparison). The prediction of k_{-3} can, thus, be improved by correcting for additional fall-off, if necessary.

Application of the ^{13}C n.m.r. Shifts in Peroxynitrates RO_2NO_2

After the parameters required for eq. (III) had been determined, tables became available which allow to estimate n.m.r. shifts from incremental values, using, e.g., the software package SpecInfo [49] which is based on the Hose code [46]. In addition, ^{13}C n.m.r. shifts of several RO_2NO_2 have recently been determined experimentally demonstrating that the calculated n.m.r. shifts are reliable (see Table V).

When the experimental activation energies for reaction (−3) at 1 bar total pressure are plotted as a function of the δ values which have been either calculated by the SpecInfo computer program or experimentally determined (see Table VI), a reasonably linear correlation results:

$$\begin{aligned} E_a,\ 1\ \mathrm{bar/kJ\ mol^{-1}} = (0.314 \pm 0.030) \\ \times (\delta/\mathrm{ppm}) + 64.0\ (2\sigma) \end{aligned} \quad \text{(VIII)}$$

The values of E_a, 1 bar calculated from eq. (VIII) are very similar to those which are derived from eqs. (III a)−(III f) after averaging the values obtained for different X. The peroxynitrates included in Table VI are essentially those from Table II, complemented by more recent data from our laboratory and by temperature dependent data on k_{-3} for additional RO_2NO_2 from other research groups. In the same way as was described in the previous section for T^* and δ_X, a linear correlation between T^* and δ can be established using the δ values from Table VI:

$$T^*/\mathrm{K} = 0.713\ \delta/\mathrm{ppm} + 199.1 \quad \text{(IX)}$$

Although the plot $T^* = f(\delta)$ is slightly curved, a linear fit according to eq. (IX) is used here for simplicity. By inserting E_a and T^* from eqs. (VIII) and (IX) into

Table IV Ratio of Calculated (k_{calc}) and Experimental (k_{exp}) Rate Constants k_{-3} for the Reactions RO_2NO_2 (+M) → RO_2 + NO_2 (+M) at Temperature T^*; k_{calc} is Calculated from Eq. (VI), T^* is the Temperature where $k_{-3,\,exp} = 3 \times 10^{-3}$ s^{-1}. This Table shows the Scatter of k_{-3} Values which are Calculated for the same RO_2NO_2 from Different RX, Errors of k_{-3} are Reduced by Averaging the Values Deduced from Different RX; Open Areas Denote RX where no δ Values were found in the Literature

R	T^* [K]	k_{calc}/k_{exp}	k_{calc}/k_{exp}	k_{calc}/k_{exp}	k_{calc}/k_{exp}	k_{calc}/k_{exp}	k_{calc}/k_{exp}	k_{calc}/k_{exp}
		X = H	X = CH_3	X = OH	X = OCH_3	X = Cl	X = F	Geometric Mean of columns 3–8
C_6H_{11}	246.5	0.24	0.22	0.34	0.25	0.16	0.26	0.24
C_2H_5	247.5	0.96	1.28	1.49	0.96	1.24	1.64	1.24
$CH_3C(O)CH_2$	249.3	0.33	0.46	0.68		0.75	0.88	0.58
CH_3	251.2	2.89	4.42	6.51	4.92	9.14	5.55	5.24
$C_6H_5CH_2$	254.7	1.35	1.28	2.40	1.50	2.13	2.24	1.76
CH_2I	258.9	27.07	23.20					25.1
$HOCH_2$	255.8	0.35	0.37	0.48	0.27			0.36
CH_3OCH_2	263.0	0.59	0.59	0.61	0.40	0.28		0.48
CH_2Cl	265.9	6.56	5.40		2.75	6.63		5.04
$CH_3C(O)OCH(CH_3)$	267.6	1.25	1.28					1.26
$C_6H_5OCH_2$	267.9	1.68						1.68
CCl_3	269.3	0.65	0.29			0.31		0.39
$(CH_3)_2NC(O)$	304.0	1.37	0.70			0.80		0.92
$CH_3OC(O)$	307.0	2.32	1.04		0.68	1.08		1.15
$C_6H_5OC(O)$	310.2		1.86			1.47		1.65
$CH_3C(O)$	311.7	0.65	0.30	0.37	0.35	0.49	0.74	0.46
$C_2H_5C(O)$	312.2	0.62	0.27	0.30	0.25			0.34
$C_6H_5C(O)$	313.1	1.17	0.53	0.87	0.57	0.68	1.56	0.92
$ClC(O)$	317.5		4.55		5.01	8.66		5.82
$CCl_3C(O)$	319.2			2.88	2.21			2.52
$CF_2ClC(O)$	321.0		2.83					2.83
$CF_3C(O)$	322.3		3.35	5.56	4.48			4.37

eq. (VII), the following Arrhenius-like expression results:

$$k_{-3} = 3 \times 10^{-3} \times \exp\{[0.314\,\delta + 64.0]/[Rx(0.713\,\delta + 199.1)]\} \times \exp\{-[(0.314\,\delta + 64.0)/RT]\}\ s^{-1}, \quad (X)$$

Table V Calculated (SpecInfo Program [49]) and Measured ^{13}C n.m.r. Shifts of the C Atom Connected to the Peroxy Group in Peroxynitrates RO_2NO_2

RO_2NO_2	$\delta_{calculated}$ [ppm]	$\delta_{experimental}$ [ppm], ref.
$CF_3O_2NO_2$	119.4 ± 1.6	123.5 [50]
$CCl_3O_2NO_2$	116.1[a]	116.1 [51]
$CH_3C(O)O_2NO_2$	167.8 ± 4.4	167.0 [52]
$C_2H_5C(O)O_2NO_2$	171.4 ± 3.5	169.2, this work
$FC(O)O_2NO_2$	144.4 ± 2.5	144.8 [53]
$CF_3C(O)O_2NO_2$	156.0 ± 2.7	155.4 [52]

[a]Experimental value (last column) has been adopted by the SpecInfo program.

where the units of δ, R, and T are ppm, kJ $mol^{-1}K^{-1}$, and K, respectively. Equation (X) is equivalent to eq. (VI) but avoids the need to average k_{-3} values for different X in order to achieve acceptable error limits. The kinetic parameters for the thermal decomposition of RO_2NO_2 as calculated with eqs. (VIII) and (X) are compared with experimental data in Table VI. The average deviation of the calculated activation energies from the experimental values is 2.8 kJ mol^{-1}. For comparison, errors for experimental activation energies are substantially larger in most cases except of very detailed investigations. The results for E_a obtained by application of eq. (VIII) are equivalent to the use of eqs. (III a)–(III f). In addition, however, eq. (VIII) also gives the correct value of E_a for $CH_2IO_2NO_2$ whereas the value calculated from eq. (III) is off by about 10 kJ mol^{-1} (see Fig. 9 for comparison).

In the last column of Table VI, rate constants calculated for 298 K are compared with experimental values [54]. The average deviation (geometric mean) is a factor of 2.2. The calculated decomposition rate constant of $CH_2IO_2NO_2$ also fits to the experimental data,

Table VI Comparison of Calculated and Experimental Kinetic Parameters for the Reactions RO_2NO_2 (+M) → RO_2 + NO_2 (+M); the Calculated Parameters are Obtained from Eqs. (VIII) and (X)

R	$\delta(^{13}C$ n.m.r.) (RO_2NO_2) [ppm]	Lit	$E_{a,\,1\,bar,\,exp.}$[a] [kJ mol^{-1}]	Lit	$E_{a,\,1\,bar,\,calc.}$[b] [kJ mol^{-1}]	$E_{a,\,calc.}$-$E_{a,\,exp.}$ [kJ mol^{-}]	$k_{calc.}/k_{exp.}$[c] at 298 K, ≈ 1 bar
C_6H_{11}	73.4 ± 2.6	SpecInfo	87.4 ± 4.8	this work	87.2	−0.2	0.42
C_2H_5	69.6 ± 0.8	SpecInfo	86.2 ± 4.0	[9]	86.0	−0.2	0.79
$CH_3C(O)CH_2$	72.9 ± 4.9	SpecInfo	88.4 ± 4.8	this work	87.1	+1.5	0.82
CF_2ClCH_2	66.0 ± 6.8	SpecInfo	90.9 ± 5.9	[39]	84.9	−6.0	1.73
$CFCl_2CH_2$	68.2 ± 6.8	SpecInfo	91.2 ± 5.3	[39]	85.4	−5.8	1.58
$C_6H_5CH_2$	71.6 ± 1.6	SpecInfo	89.8 ± 4.8	this work	86.7	−3.1	1.30
CH_3	61.9 ± 2.9	SpecInfo	83.8 ± 5.9	[9]	83.6	−0.2	3.61
C_3H_7	68.6 ± 0.8	SpecInfo	82.8	[55]	85.7	+2.9	2.09
$HOCH_2$	98.0 ± 18.2	SpecInfo	85.3[a,e]	[40]	94.9	+9.6	0.18
CH_2I	89.5 ± 4.4	SpecInfo	91.8 ± 4.9	this work	92.3	+0.5	0.53
CH_3OCH_2	95.7 ± 1.8	SpecInfo	93.5 ± 5.4	[41]	94.2	+0.7	0.51
CH_2Cl	88.0 ± 4.4	SpecInfo	91.7 ± 2.9	[7]	91.8	+0.1	1.89
$CH_3C(O)OCH(CH_3)$	99.8 × 3.4	SpecInfo	94.9 ± 5.1	this work	95.5	+0.6	0.67
$C_6H_5OCH_2$	95.6 ± 1.6	SpecInfo	95.0 ± 5.2	this work	94.2	−0.8	1.06
CCl_3	116.1	[50]	96.8 ± 1.4	[10]	100.6	+3.8	0.16
CCl_2F	122.3 ± 4.7	SpecInfo	100.3 ± 1.8	[10]	102.6	+2.3	0.25
CF_3	123.5	[51]	96.8 ± 1.4	[55]	101.7	+4.0	0.51
$CClF_2$	111.2 ± 5.4	SpecInfo	98.7 ± 1.8	[10]	99.1	+0.4	1.24
$(CH_3)_2NC(O)$	153.3 ± 4.8	SpecInfo	111.5 ± 5.8	this work	112.4	+0.9	0.53
$CH_3OC(O)$	154.8 ± 2.0	SpecInfo	107.0 ± 4.5	[41]	112.8	+5.8	0.66
t-$C_4H_9OC(O)$	154.8 ± 2.0	SpecInfo	111.6 ± 4.7	[41]	112.8	+1.2	0.45
$C_6H_5OC(O)$	154.8 ± 2.0	SpecInfo	112.7 ± 4.5	this work	112.8	+2.8	1.06
$CH_3C(O)$	167.0	[52]	112.9 ± 1.9	[42,43]	116.7	+3.8	0.37
$C_2H_5C(O)$	169.2	this work	115.9 ± 2.2	this work	117.3	+1.4	0.34
$C_6H_5C(O)$	164.6 ± 0.7	SpecInfo	116.4 ± 3.8	this work	115.9	−0.5	0.63
$CH_2{=}C(CH_3)C(O)$	154.5 ± 2.5	SpecInfo	112.1 ± 4.2	[57]	112.7	+0.6	1.59
$ClC(O)$	158 ± 21	SpecInfo	115.1 ± 3.2	[44]	113.8	−1.3	2.27
$FC(O)$	144.8	[53]	116.0^{+15}_{-23}	[58]	109.5	−6.5	9.74
$CCl_3C(O)$	160.2 ± 3.3	SpecInfo	120.6 ± 5.2	[39]	114.5	−6.1	2.62
$CFCl_2C(O)$	162.4 ± 0.6	SpecInfo	118.0 ± 5.2	[39]	115.2	−2.8	1.99
$CF_2ClC(O)$	161.3 ± 2.6	SpecInfo	118.6 ± 5.2	[39]	114.9	−3.7	2.86
$CF_3C(O)$	155.4	[52]	119.1 ± 5.0	[39]	113.0	−6.1	6.45

[a]Activation energies are the same as in Table II, or, for the new entries, from the original articles cited in column 5.
[b]Activation energies are calculated from eq. (VIII).
[c]$k_{calc.}$ is calculated from eq. (X), $k_{exp.}$ is the same as in Table II, or, for the new entries, taken from the original articles cited in column 5.

different from the application of eq. (VI) and the parameters of Table III (see Table IV for comparison). There appears to be a systematic overestimation of k_{-3} for halogenated formyl and acetyl peroynitrates and a systematic underestimation of the nonhalogenated acetyl peroxynitrates by the calculations. For this reason, it will be preferable to adopt the experimental k_{-3} values of PAN also for other acyl peroxynitrates of the structure $R(R')(R'')C(O)O_2NO_2$, as was already suggested by Roberts [3], as long as R, R′, and R″ are not particularly strongly electron drawing substituents.

In Figure 10, the experimental k_{-3} values at 298 K are plotted as a function of δ. A linear fit to the data points results in:

$$\log(k_{-3,298}\ \mathrm{k/s^{-1}}) = -0.0443 \times \delta/\mathrm{ppm} + 3.59 \quad \text{(XI)}$$

Since the data points for the peroxynitrates of intermediate stability tend to be above the least-squares line of the linear fit (see Fig. 10), a quadratic expression reproduces the data slightly better, resulting in

$$\log(k_{-3,298}/\mathrm{s^{-1}}) = -0.000182 \times (\delta/\mathrm{ppm})^2 - 0.0016 \times \delta/\mathrm{ppm} + 1.36 \quad \text{(XII)}$$

Equations (X)–(XII) can be used to predict rate constants for the decomposition of peroxynitrates when

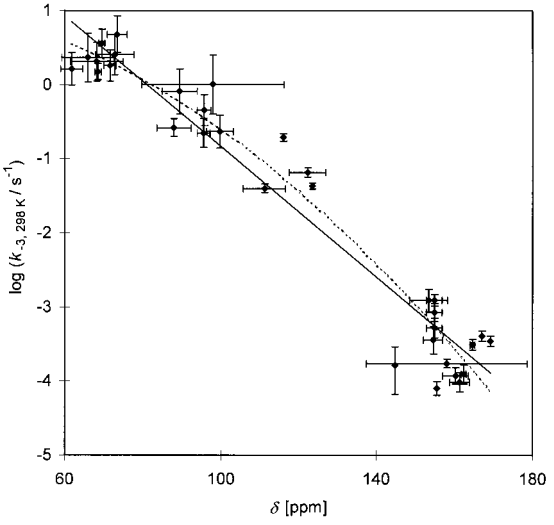

Figure 10 Correlation between experimental decomposition rate constants k_{-3} of RO_2NO_2 at 298 K, 1 bar (M = N_2) and the ^{13}C n.m.r. shifts of the carbon atom connected to the peroxy group in RO_2NO_2; error bars of δ are output of the SpecInfo program and are related to the volume and consistency of the data base of that program; error bars of *k* are taken or deduced from the original articles.

there are no experimental data available. This procedure can be useful to estimate the thermal lifetimes of new peroxynitrates which are either of potential interest for the atmosphere or can be formed from intermediate RO_2 radicals in laboratory investigations on the degradation of hydrocarbons in the presence of NO_X. In Table VII, decomposition rate constants have been calculated for a number of peroxynitrates of potential interest for which there are no experimental data available.

Discussion of Table VII

Several interesting aspects of the data in Table VII will now be discussed. There have been early attempts to generate $HC(O)O_2NO_2$, the simplest acyl peroxynitrate. IR bands originally assigned to $HC(O)O_2NO_2$ [63] were subsequently recognized to belong to HO_2NO_2 [64,65]. According to Table VII, this peroxynitrate should also be quite stable at room temperature. The difficulties to generate $HC(O)O_2NO_2$ probably arise from the thermal instability of the $HCO \cdot O_2$ addition product which falls apart at room temperature and atmospheric pressure before it can add NO_2. Attempts in this laboratory to isolate $HC(O)O_2NO_2$ at lower temperatures [66] also failed. Possibly, $HC(O)O_2NO_2$ can be generated at much higher total pressures where both addition processes, reactions (2) and (3), are closer to the high-pressure limit. Other peroxynitrates which are quite stable according to Table VII and could be generated in the atmosphere, are $HC(O)C(O)O_2NO_2$ and $CH_3C(O)C(O)O_2NO_2$. Here again, attempts to generate $HC(O)C(O)O_2NO_2$ [66] and $CH_3C(O)C(O)O_2NO_2$ [66,67] were unsuccessful, also at temperatures below room temperature [66]. This can possibly be explained by the thermal instability of the intermediate RC(O)C(O) radicals (R = H, CH_3) with respect to splitting off a CO molecule [66,67].

Another interesting compound is $C_6H_5O_2NO_2$ which, according to Table VII, should be thermally stable enough to be detected in smog chamber experiments. Attempts to generate $C_6H_5O_2NO_2$ from benzene [6] failed. Here, either: (i) the phenylperoxy radical is thermally very unstable, or; (ii) there is a potential barrier for the addition of O_2 to C_6H_5, or; (iii) the O—O bond in the peroxynitrate is weaker than the OO—N bond, thus, giving C_6H_5O and NO_3 as decomposition products rather than $C_6H_5O_2$ and NO_2.

Recent measurements of the rate constant of reaction (16),

$$C_6H_5 + O_2\ (+M) \rightarrow C_6H_5O_2\ (+M), \qquad (16)$$

as a function of temperature between 297 and 815 K [68,69] show that (i) and (ii) are unlikely. On the other hand, more recent ab initio calculations on the heat of reaction for the addition of O_2 to the phenyl radical (-171.5 kJ mol^{-1} [70]) combined with the heats of formation of phenyl (339 kJ mol^{-1} [71]), phenoxy (54 kJ mol^{-1} [71]), NO_2 [72], NO_3 [72], and an estimated OO—NO_2 bond energy in $C_6H_5O_2NO_2$ of 117 kJ mol^{-1} from Table VII suggest that the bond energy in $C_6H_5O_2NO_2$ with respect to reaction (17),

$$C_6H_5O_2NO_2\ (+M) \rightarrow C_6H_5O + NO_3\ (+M), \qquad (17)$$

is $\approx$ 30 kJ mol^{-1}. Since there is no obvious reason for a notable barrier of reaction (17) in addition to the reaction enthalpy, $C_6H_5O_2NO_2$ is probably thermally unstable even at room temperature and in the presence of NO_2 due to reaction (17).

According to Table VII, a number of relatively stable acyl peroxynitrates can be formed during the atmospheric degradation of biogenic compounds under NO_X-rich conditions. Finally, Table VII suggests that $CH_3C(S)O_2NO_2$ (thioacetyl peroxynitrate) might be a thermally particularly stable peroxynitrate.

Table VII Rate Parameters for the Thermal Decomposition of Peroxynitrates as Predicted by Application of Eqs. (VIII) and (X)[a]

RO_2NO_2	^{13}C n.m.r. shift δ (SpecInfo) [ppm]	$k_{298\ K,\ calc.}$ [s^{-1}]	$A_{1\ bar,\ calc.}$ [$10^{16}\ s^{-1}$]	$E_{a,\ 1\ bar,\ calc.}$[b] [kJ mol^{-1}]	Precursor(s), Ref.[c] [kJ mol^{-1}]
$CH_3SCH_2O_2NO_2$	71.6 ± 0.6	2.4	0.34	86.5	CH_3SCH_3 [59,60]
$(CH_3)_2NCH_2O_2NO_2$	75.5 ± 5.5	1.7	0.39	87.7	$(CH_3)_3N$
Cyclohexanone-2-nitrate-3-peroxynitrate	81.8 ± 3.5	0.90	0.47	89.7	Cyclohexanone-2-nitrate [61]
trans-2,3-Dinitrooxo-3-methyl-cyclohexyl peroxynitrate	84.0 ± 0.6	0.73	0.50	90.4	trans-1-methyl-cyclo-hexyl-1,2-dinitrate [61]
$O_2NOCH_2C(H)(Cl)O_2NO_2$	86.1 ± 4.7	0.60	0.54	91.0	CH_2═CHCl [62]
$O_2NOC(H)(Cl)(H)ClO_2NO_2$	88.4 ± 4.7	0.48	0.58	91.7	CHCl═CHCl [62]
$CH_2BrO_2NO_2$	89.5 ± 4.4	0.43	0.59	92.1	CH_3Br
$CF_3CCl_2O_2NO_2$	98.2 ± 3.7	0.18	0.76	98.8	CF_3CCl_2H
$O_2NOCH_2CCl_2O_2NO_2$	98.2 ± .37	0.18	0.76	94.8	CH_2═CCl_2 [62]
$O_2NOC(H)(Cl)CCl_2O_2NO_2$	100.1 ± 3.7	0.15	0.80	95.4	CH_2═CCl_2 [62]
N≡C—O_2NO_2	109.4 ± 0.8	0.059	1.04	98.4	HCN
$CH_2FO_2NO_2$	111.5 ± 5.4	0.048	1.10	99.0	CH_3F
$CF_3CFClO_2NO_2$	112.0 ± 7.7	0.046	1.11	99.2	CF_3CClFH
$HC(O)OC(O)O_2NO_2$	149.9 ± 2.4	0.00093	2.7	111.1	HC(O)OC(O)H
CH_2═$C(H)O_2NO_2$	151.1 ± 2.2	0.00082	2.8	111.5	
$CH_3OCH_2OC(O)O_2NO_2$	154.8 ± 2.0	0.00055	3.0	112.6	
$HC(O)C(O)O_2NO_2$	159.8 ± 2.4	0.00033	3.4	114.2	isoprene, aromatics
CH_3N═CO_2NO_2	161.3 ± 7.6	0.00028	3.5	115.6	$(CH_3)_3N$
$HC(O)O_2NO_2$	162.0 ± 1.5	0.00026	3.5	114.9	
$CH_3C(O)C(O)O_2NO_2$	163.1 ± 2.1	0.00023	3.6	115.2	isoprene, aromatics
$HOCH_2C(CH_3)$═$C(H)C(O)O_2NO_2$	164.5 ± 0.5	0.00020	3.7	115.6	isoprene
$C_6H_5O_2NO_2$	165.8 ± 0.4	0.00017	3.8	116.1	$C_6H_5CH_3$
$HOCH_2C(O)O_2NO_2$	167.5 ± 1.1	0.00014	3.9	116.6	isoprene
$HOCH_2C(H)$═$C(CH_3)C(O)O_2NO_2$	168.2 ± 0.6	0.00013	4.0	116.8	isoprene
$HOCH_2C(CH_3)(OH)C(O)O_2NO_2$	172.4 ± 5.4	0.000085	4.3	118.2	isoprene
$C(H)(O)C(CH_3)(OH)C(O)O_2NO_2$	173.0 ± 1.2	0.000080	4.4	118.3	isoprene
$CH_3C(S)O_2NO_2$	196.0 ± 36.2	0.000007	6.7	125.5	

[a]To our knowledge, experimental data on the kinetic parameters of these reactions are presently not available in the literature.

[b]The error arising for E_a from the linear regression $E_a(\delta)$ is ± 4.0 kJ mol^{-1} (2σ).

[c]In the given references, experimental evidence has been obtained that the peroxynitrate is formed during the degradation of the stated precursor molecule under laboratory conditions.

*Note added in proof: Recently (Sehested et al., Int J Chem Kinet 30, 475, 1998) published thermal decomposition rate constants k-3 of acetonyl peroxynitrate at 1bar are in excellent agreement with the results of this work (lower by 14% at 250 K, 6% at 298 K).

SUMMARY

Summarizing, it is proposed that for estimating k_{-3} values of new peroxynitrates eq. (VI) can be used if the SpecInfo program is not accessible, and eq. (X) can be used in case SpecInfo or something equivalent is available. For a quick estimate of k_{-3} for a certain RO_2NO_2, appropriate classification in Table II with respect to the chemical nature of R, in particular to its electron withdrawing potential, will be useful.

Financial support of this work by the EC (European Commission) under contract no. EV5V-0024 and by the Bundesminister für Bildung, Wissenschaft, Forschung und Technologie (BMBF) is gratefully acknowledged. The authors would like to thank Dr. G. Hirsch, Wuppertal, for MNDO calculations of the vibrational frequencies of propionyl peroxynitrate.

BIBLIOGRAPHY

1. Nielsen, T.; Samuelsson, U.; Grennfelt, P.; Thomsen, E. L. Nature 1981, 293, 553.
2. Singh, H. B. Environ Sci Technol 1987, 21, 320.
3. Roberts, J. M. Atmos Environ 1990, 24A, 243.
4. Lightfoot, P. D.; Cox, R. A.; Crowley, J. N.; Destriau,

M.; Hayman, G. D.; Jenkin, M. E.; Moortgat, G. K.; Zabel, F. Atmos Environ 1992, 26A, 1805.
5. Zabel, F. Thermischer Zerfall von Peroxynitraten; Habilitation Thesis: Wuppertal, Germany, 1993.
6. Kirchner, F. Kinetische Untersuchungen an Peroxynitraten und Peroxy-Radikalen; Ph. D. Thesis: Wuppertal, Germany, 1993.
7. Zabel, F. Z Phys Chem 1995, 188, 119.
8. Bahta, A.; Simonaitis, R.; Heicklen, J. J Phys Chem 1982, 86, 1849.
9. Zabel, F.; Reimer, A.; Becker, K. H.; Fink, E. H. J Phys Chem 1989, 93, 5500.
10. Köppenkastrop, D.; Zabel, F. Int J Chem Kinet 1991, 23, 1.
11. Barnes, I.; Becker, K. H.; Fink, E. H.; Reimer, A.; Zabel, F.; Niki, H. Int J Chem Kinet 1983, 15, 631.
12. Diehl, J. W.; Finkbeiner, J. W.; DiSanzo, F. P. Anal Chem 1995, 67, 2015.
13. Derwent, R. G.; Jenkin, M. E. Atmos Environ 1991, 25A, 1661.
14. Singh, H. B.; Salas, L. J.; Cantrell, B. K.; Redmond, R. M. Atmos Environ 1985, 19, 1911.
15. Haszpra, L.; Szilagyi, I.; Demeter, A.; Turanyi, T.; Berces, T. Atmos Environ 1991, 25A, 2103.
16. Atkinson, R.; Aschmann, S. M.; Carter, W. P. L. Int J Chem Kinet 1989, 21, 801.
17. Wallington, T. J.; Skewes, L. M.; Siegl, W. O. J Photochem Photobiol A: Chem 1988, 45, 167.
18. Ohta, T.; Mizoguchi, I. Environ Sci Technol 1981, 15, 1229.
19. Kenley, R. A.; Hendry, D. G. J Am Chem Soc 1982, 104, 220.
20. Kirchner, F.; Zabel, F.; Becker, K. H. Chem Phys Lett 1992, 191, 169.
21. Chameides, W. L.; Davis, D. D.; J Geophys Res 1980, 85, 7383.
22. Solomon, S.; Garcia, R. R.; Ravishankara, A. R. J Geophys Res 1994, 99, 20491.
23. Klick, S.; Abrahamsson, K. J Geophys Res 1992, 97, 12683.
24. Schmitt, G.; Comes, F. J. J Photochem 1980, 14, 107.
25. In the $CH_2I_2/O_2/N_2 + h\nu(300\ nm)$ reaction system of ref. [24], the increased reformation of CH_2I_2 in the presence of O_2 can possibly be explained as well by the more conventional reaction scheme $CH_2IO_2 + CH_2IO_2 \rightarrow CH_2IO + CH_2IO + O_2$, followed by $CH_2IO\ (+M) \rightarrow CH_2O + I\ (+M)$ and $CH_2I + I\ (+M) \rightarrow CH_2I_2\ (+M)$. The appearance of CH_2OO biradicals which were proposed in ref. [24] should lead to anomalies in the product distribution. However, typical peroxynitrate bands were observed at 1736, 1300, and 787 cm^{-1} in addition to a band at 989 cm^{-1}, and the time dependence of these IR bands was completely analogeous to those observed in many other reaction systems where peroxynitrates are formed after the preparation of substituted alkyl radicals in the presence of both O_2 and NO_2.
26. Singh, H. B.; O'Hara, D.; Herlth, D.; Bradshaw, J.; Sandholm, S. T.; Gregory, G. L.; Sachse, G. W.; Blake, D. R.; Crutzen, P. J.; Kanakidou, M. A. J Geophys Res 1992, 97, 16511.
27. Grosjean, D.; Williams, II, E. L.; Grosjean, E. Environ Sci Technol 1993, 27, 110.
28. Nielsen, T.; Hansen, A. M.; Thomsen, E. L. Atmos Environ 1982, 16, 2447.
29. D'Ans, J.; Frey, W. Chem Ber 1905, 45, 1845.
30. Gaffney, J. S.; Fajer, R.; Senum, G. I. Atmos Environ 1984, 18, 215.
31. Mayer-Figge, A. Untersuchungen am Propionylperoxinitrat, Diplom Thesis: Wuppertal, Germany, 1993.
32. Troe, J. J Phys Chem 1979, 83, 114.
33. MNDO calculations were performed using the program MNDO/91 from Dewar et al. (ref. [34]). The frequencies calculated by this program were scaled using model substances like CH_3ONO_2 for which experimental frequencies are available.
34. Dewar, M. J. S.; Ford, G. P.; McKee, M. L.; Rzepa, H. S.; Thiel, W.; Yamaguchi, Y. J Mol Struct 1978, 43, 135.
35. Schurath, U.; Wipprecht, V. Reaction of Peroxyacyl Radicals; in 1st European Symposium on Physico-Chemical Behaviour of Atmospheric Pollutants, Versino, B.; Ott, H. Eds., Commission of the European Communities: Bruxelles, 1979; pp. 157–166.
36. Grosjean, D.; Grosjean, E.; Williams, II, E. L. J Air Waste Manage Assoc 1979; 44, 391.
37. Mineshos, G.; Glavas, S. React Kinet Catal Lett 1991, 45, 305.
38. Singh, H. B.; Chen, Y.; Gregory, G. L.; Sachse, G. W.; Talbot, R.; Blake, D. R.; Kondo, Y.; Bradshaw, J. D.; Heikes, B.; Thornton, D. Geophys Res Lett 1997, 24, 127.
39. Zabel, F.; Kirchner, F.; Becker, K. H. Int J Chem Kinet 1994, 26, 827.
40. Barnes, I.; Becker, K. H.; Fink, E. H.; Reimer, A.; Zabel, F. Chem Phys Lett 1985, 115, 1.
41. Kirchner, F.; Thüner, L. P.; Barnes, I.; Becker, K. H.; Donner, B.; Zabel, F. Environ Sci Technol 1997, 31, 1801.
42. Bridier, I.; Caralp, F.; Loirat, H.; Lesclaux, R.; Veyret, B.; Becker, K. H.; Reimer, A.; Zabel, F. J Phys Chem 1991, 95, 3594.
43. Evaluation in ref. [7] of the data from Bridier et al. [42].
44. Kirchner, F.; Libuda, H. G.; Zabel, F. 11th International Symposium on Gas Kinetics; Book of Abstracts: Assisi, 1990; p. A3.
45. Parlar, H.; Kotzias, D.; Herrman, M.; Zsolnay, A. Chemosphere 1986, 15, 971.
46. Bremser, W.; Franke, B.; Wagner, H. Chemical Shift Ranges in Carbon-13 NMR Spectroscopy; VCH: Weinheim, Germany, 1982.
47. Most of the δ values from ref. [46] which were used to derive the coefficients in eqs. (III) and (IV) are tabulated in ref. [6]. For the present work, the data base of ref. [6] has been complemented by more recent δ values for several additional R; for this reason, the coefficients a_X, b_X, c_X, and d_X in this work are slightly different from those of ref. [6].

48. Wehrli, F.; Wirthlin, T. Interpretation of Carbon-13 Nuclear Magnetic Resonance Spectra; Heyden & Son Ltd.: London, 1976.
49. Software package SpecInfo; Chemical Concepts GmbH: Weinheim, 1996.
50. Gäb, S.; Turner, W. V. Angew Chem 1985, 97, 48.
51. Kopitzky, R.; Willner, H. private communication, 1997.
52. Kopitzky, R.; Beuleke, M.; Balzer, G.; Willner, H. Inorg Chem 1997, 36, 1994.
53. Scheffler, D.; Schaper, I.; Willner, H.; Mack, H.-G.; Oberhammer, H. Inorg Chem 1997, 36, 339.
54. If the experimental temperature range does not include 298 K, the rate constant at 298 K is obtained by extrapolation using the Arrhenius expression recommended in the original article.
55. Edney, E. O.; Spence, J. W.; Hanst, P. L. J Air Poll Control Assoc 1979, 29, 741.
56. Mayer-Figge, A.; Zabel, F.; Becker, K. H. J Phys Chem 1996, 100, 6587.
57. Roberts, J. M.; Bertman, S. B. Int J Chem Kinet 1992, 24, 297.
58. Bednarek, G.; Arguello, G. A.; Zellner, R. Ber Bunsenges Phys Chem 1996, 100, 445.
59. Jensen, N. R.; Hjorth, J.; Lohse, C.; Skov, H.; Restelli, G. Atmos Environ 1991, 25A, 1897.
60. Nielsen, O. J.; Sehested, J.; Wallington, T. J. Chem Phys Lett 1995, 236, 385.
61. Wängberg, I.; Barnes, I.; Becker, K. H. Chem Phys Lett 1996, 261, 138.
62. Noremsaune, I. M. W.; Hjorth, J.; Nielsen, C. J. J Atmos Chem 1995, 21, 223.
63. Gay, B. W. Jr.; Noonan, R. C.; Bufalini, J. J.; Hanst, P. L. Environ Sci Technol 1976, 10, 82.
64. Hanst, P. L.; Gay, Jr., B. W. Environ Sci Technol 1977, 11, 1105.
65. Niki, H.; Maker, P. D.; Savage, C. M.; Breitenbach, L. P. Chem Phys Lett 1977, 45, 564.
66. Mayer-Figge, A. Thermischer Zerfall von Peroxynitraten verschiedener Struktur: Experimentelle Untersuchungen und Berechnungen; Ph. D. Thesis: Wuppertal, Germany, 1997.
67. Tyndall, G. S.; Staffelbach, T. A.; Orlando, J. J.; Calvert, J. G. Int J Chem Kinet 1995, 27, 1099.
68. Yu, T.; Lin, M. C. J Am Chem Soc 1994, 116, 9571.
69. Schaugg, J. Untersuchung der Reaktion von Phenyl mit molekularem Sauerstoff in einem Strömungsreaktor; Ph. D. Thesis: Stuttgart, Germany, 1997.
70. Mebel, A. M.; Lin, M. C. J Am Chem Soc 1994, 116, 9577.
71. Tsang, W. Heats of Formation of Organic Free Radicals by Kinetic Methods in Energetics of Organic Free Radicals, Martinho Simoes, J. A.; Greenberg, A.; Liebman, J. F. Eds., Blackie Academic and Professional: London, 1996; pp. 22–58.
72. DeMore, W. B.; Sander, S. P.; Golden, D. M.; Hampson, R. F.; Kurylo, M. J.; Howard, C. J.; Ravishankara, A. R.; Kolb, C. E.; Molina, M. J. Chemical Kinetics and Photochemical Data for Use in Stratospheric Modeling; Evaluation No. 12, JPL Publication 97-4: Pasadena, 1997.